ISTITUTO NAZIONALE DI FISICA NUCLEARE

Sezione di Trieste

INFN/TC-89/5

20 luglio 1989

C. Tuniz, R. Devoti, G. Santoro and F. Zanini

A SYNCHROTRON RADIATION MICROPROBE FOR X-RAY FLUORESCENCE AND MICROTOMOGRAPHY AT ELETTRA. APPLICATIONS IN LIFE SCIENCE

Servizio Documentazione
dei Laboratori Nazionali di Frascati

Presented at the
"2nd International Workshop on XRF and PIXE Applications in Life Science"
Capri (Italy);June 29-30, 1989.

A SYNCHROTRON RADIATION MICROPROBE FOR X-RAY FLUORESCENCE AND MICROTOMOGRAPHY AT ELETTRA. APPLICATIONS IN LIFE SCIENCE

CLAUDIO TUNIZ and ROBERTO DEVOTI
Dipartimento di Fisica, Università di Trieste, and I.N.F.N., Sezione di Trieste
Via A. Valerio 2, 34127 Trieste, Italy

GIUSEPPE SANTORO
Scuola Normale Superiore, Piazza dei Cavalieri 7, 56100 Pisa, Italy

and

FRANCO ZANINI
Sincrotrone Trieste, Padriciano 99, 34012 Trieste, Italy

ABSTRACT

A synchrotron radiation microscope based on X-ray fluorescence and computed microtomography for advanced applications in life science is described. This microscope will utilize the radiation produced by a bending magnet of ELETTRA, the third generation, high brilliance synchrotron radiation facility being built in Trieste. Various mirror systems, operating in an energy range between 7 and 17 keV, with white and monochromatic light, have been designed. For example, multilayer coated mirrors in the Kirkpatrick-Baez configuration can produce a spatial resolution of 1 μm^2 for a flux in excess of 10^8 photons per second on the sample ($E = 12$ keV, $E/\Delta E = 10$). This X-ray microprobe will allow micrometric mapping of trace and minor elements and computed tomographic imaging in biological materials with high resolution, opening a new realm of experiments in life science such as *in vivo* elemental scanning of cultured cells and microtomographic analysis of histological samples. The preliminary design of the beamline, the performance of the microprobe and its use in life science are discussed.

1. Introduction

Various analytical procedures have been developed in recent years for improved detection of trace elements for applications in life science. Nuclear and atomic techniques have the advantage of allowing fast, non-destructive, and multielemental analyses. Successful results have been obtained with methods based on the measurement of characteristic X-rays (fluorescence) emitted by the element of interest. These X-rays have energies in the range of up to a few tens of keV and are detected with solid state detectors (*e.g.* Si(Li)). Fluorescence emission follows the production of holes in the K-, L- and M-shells of atoms by MeV protons from particle accelerators (PIXE: Proton Induced X-ray Emission) or X-ray photons (XRF: X-Ray Fluorescence).

One advantage of using X-rays rather than protons or electrons is that they deposit in the sample a small amount of energy for a given fluorescence signal. A second is that selectivity can be greatly enhanced by resonant absorption using monochromatic X-rays. Conventional sources of photons are radioisotopes (such as ^{241}Am and ^{55}Fe) and X-ray tubes. These are weak fluorescence sources and only in particular cases can a detection limit down to the ppmw (part-per-million-weight) level be obtained.

The use of Synchrotron Radiation (SR) to induce X-ray Emission (SRIXE) for analitical purpose allows the measurement of trace elements at levels not detectable with traditional microanalytical techniques. The main advantages of SRIXE over conventional XRF based on X-ray tubes and radioisotopes are tunability of energy, high brilliance and polarization of X-rays. As explained below, the polarization allows a significant reduction of Rayleigh and Compton scattering contribution to the background. The high intensity and superior collimation of SR beams can be exploited to develop X-ray fluorescence microprobes for the analysis of very small specimens. It was recently shown that SRIXE can be used to measure femtogram quantities of specific elements within 100 μm^2 beam spots[1]. Preliminary measurements in biological samples have already shown the potential of this probe[2]. Improved mirror technology will give in the near future beam spots of a few μm^2 without loss of X-ray flux.

In approaching the optical design for a SRIXE microprobe we have to consider some constraints: the size and quality of the spot, which are responsible for the spatial resolution; the monochromaticity of the beam, which determines the element sensitivity of the system; and the X-ray flux, which sets the detection limit of the probe[3]. When applied to SRIXE, the most important parameter of the photon source is the number of photons per unit area per second. It is then clear that a third generation high brilliance ring, *i.e.* characterized by a high number of photons/second/solid angle/source area, will guarantee better performance than existing machines. In other words, since the spatial resolution of a microbeam is almost completely determined by the optical configuration of the focusing system (to a first approximation X-rays are not scattered before the fluorescence event), we can achieve high spatial resolution with little or no use of slits or pinholes, but by means of a strongly demagnifying optical configuration.

On this basis we will address some preliminary design considerations for an X-ray microbeam from the bending magnet of ELETTRA, the high brilliance synchrotron radiation facility to be built in Trieste. The characteristics of the source are described in Table I. A SR microscope based on X-ray fluorescence and computed tomography for advanced applications in life sciences will also be discussed.

Table I. Characteristics of the bending magnet source at ELETTRA.

Horizontal beam size (σ_x)	0.061	mm
Vertical beam size (σ_y)	0.086	mm
Horizontal divergence ($\sigma_{x'}$)	0.193	mrad
Vertical divergence ($\sigma_{y'}$)	0.011	mrad
Electron beam energy	2	GeV
Current	400	mA
Magnetic radius	5.5	m
Magnetic field	1.2	T
Critical energy	3.2	keV
Power density	42	W/mrad^2

2. The microbeam

2.1. Energy range

The bending magnet produces a continuum spectrum of the radiation from wich we can choose different excitation methods for X-ray fluorescence. While the continuum excitation method[4] is sensitive over a broad range of energies and is a good choice for survey measurements, a monochromatic excitation[5] gives a better signal to noise ratio.

Fluorescence efficiency is directly related to the excitation energy, so a monochromatic line just above the absorption edge would excite a single element most effectively, but such a technique suffers from a poor excitation intensity. If we use a wider energy band, we enhance the fluorescence signal of the element, but while the fluorescence signal reaches a level of saturation, the scattered radiation from light elements keeps increasing linearly, thus reducing the signal to background ratio.

To achieve higher sensitivity in both relative concentration and absolute amount, a good compromise is the application of wide band pass monochromators such as the multilayer coated mirrors system[6]. This class of devices may achieve a Minimum Detection Limit (MDL) in relative concentration better than that of the SR continuum excitation, approaching that of monochromatic excitation (*i.e.* using a traditional crystal monochromator). The MDL in absolute amount, on the other hand, is likely to be enhanced by an order of magnitude with respect to continuum excitation and by two orders with respect to monochromatic excitation.

We recall here that one of the main advantages of synchrotron radiation as a source of X-rays for fluorescence experiments is the strong polarization: for emission in the orbit plane the electric vector lies in the plane and is normal to the emission direction. Therefore a solid state detector, positioned in the horizontal plane at

90° to the direction of the incoming beam, will minimize the contribution of the Compton and Rayleigh scattered radiation to the background, for a better signal to noise ratio. The polarization characteristics of the photon source should be taken into account when designing the focusing device.

2.2. Design of a white light beamline

As a focusing device for a white light beam, we considered two different optical configurations: an ellipsoid of revolution and a Kirkpatrick-Baez (KB) system. The advantage of the ellipsoid is that low–order aberrations set no limits to its angular acceptance[7]. The practical limit we face is the size in which an elliptical surface can be fabricated at present while maintaining a correct curvature and a high level of smoothness[3]. The size of mirror is a consequence of the need to demagnify a bending magnet source (of order 100 μm) in order to obtain a lateral resolution of few microns (keeping in mind that total reflection for hard X–rays means incidence angles of few mrad).

The Kirkpatrick-Baez configuration[8] uses two cylindrical mirrors whose meridian planes are crossed, so that the sagittal rays become the tangential rays for the second mirror, and with such a system it is possible to obtain a strong demagnification and a stigmatic image. Since we are dealing with grazing angles of incidence, the cylindrical surfaces can be well approximated by spherical mirrors. We immediately see that one of the important characteristics of the KB system is that it is based on optical surfaces that can be fabricated with a high degree of accuracy and smoothness; but the presence of spherical surfaces will also mean the occurrence of spherical aberration, directly proportional to the angular acceptance of the system. This is the main limit of the Kirkpatrick-Baez system, but we will later see that multilayer coated mirrors reduce this aberration[6].

2.3. Design of a multilayer wide band pass beamline

Multilayer coated X-ray optics, where reflectivities are enhanced by causing multiple reflections to add in phase[9], present additional advantages with respect to metal coated ones: a multilayer mirror will present the same high-energy cutoff as a traditional mirror at a glancing angle up to three times larger[6]. This means not only that we will obtain the same demagnification with a smaller value of spherical aberration, the curvature of the mirror being smaller, but also that we will have the same angular acceptance with shorter (*i.e.* less expensive and more accurate) mirrors. The main disadvantage of such a configuration is the need of different coating parameters to optimize the fluorescence efficiency for different elements, so we designed three interchangeable KB systems for three energy ranges of particular interest.

The optical parameters of a Kirkpatrick-Baez system are calculated by solving the Coddington equations for both mirrors, while the characteristics of the multilayer coatings (in this case tungsten-carbon on a quartz substrate) have to take into account the central energy and the glancing angle of the microbeam and should be optimized in terms of reflectivity of the mirrors and energy bandwidth. We calculated these parameters for three different energies (7, 12 and 17 keV). Other important parameters are the demagnification of the source and the distance between the KB mirrors and the sample. This distance should be the smallest possible in order to minimize the magnification, but has to be large enough to accomodate the ionization chamber for flux normalization and the last collimating pinhole.

Figure 1, Table II and Table III illustrate the parameters for the SRIXE beamline, where R is the radius of the mirrors and d_1, d_2, θ_1 and θ_2 are the multilayer d-spacings and the incidence angles of the two mirrors M1 and M2 respectively at three different energies. To check out these parameters, we performed a ray-tracing study using the program SHADOW[10], developed by Franco Cerrina at the University of Wisconsin. The simulation takes into account a realistic bending magnet source with the parameters of ELETTRA, the real behavior of the multilayer coatings and the flux losses determined by an entrance slit placed before the KB system (in order to define a stable photon source), by the mirror dimensions and by a collimating pinhole placed between the KB system and the sample.

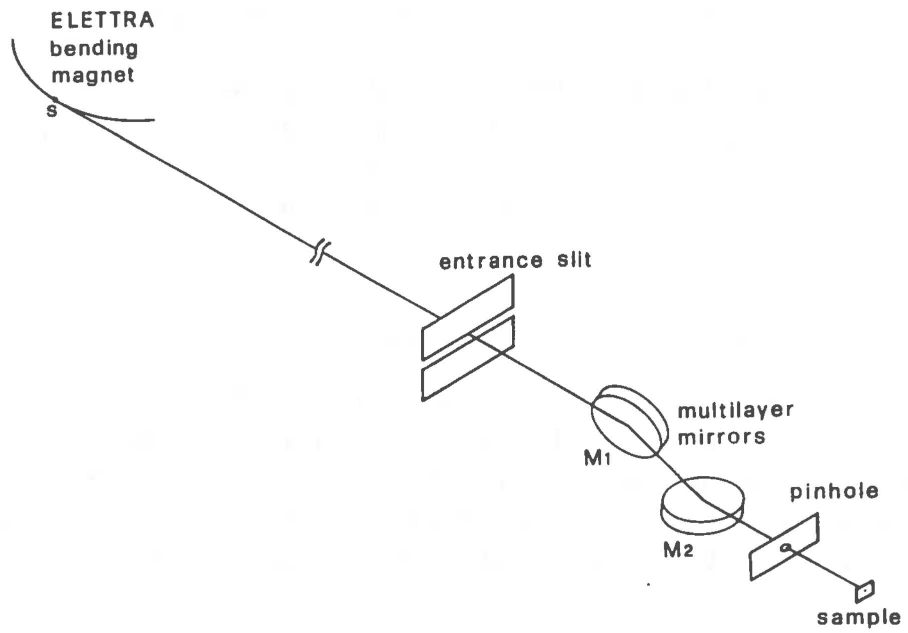

Figure 1. Schematics showing the KB focusing stage.

Table II. Optical characteristics of the beamline.

Source to slit distance	18 m
Slit to M1 distance	2 m
M1 to M2 distance	10.2-13 cm
M2 to image distance	30 cm
M1 magnification	1/50

Table III. Parameters of the Kirkpatrick-Baez focusing system at different energies.

Energy	Bandwidth	R	d_1	d_2	θ_1	θ_2
7 keV	0.6 keV	26.7 m	28 Å	40 Å	1.81°	1.27°
12 keV	1.2 keV	43.4 m	28 Å	38 Å	1.06°	0.79°
17 keV	1.5 keV	53.8 m	25 Å	33 Å	0.84°	0.63°

Table IV gives the photon fluxes on the sample at different energies and spot sizes calculated with the given parameters.

Table IV. X-ray fluxes (photons/s) on the sample at different energies and spot sizes.

Energy	100 μm^2	10 μm^2	1 μm^2
7 keV	$4{\cdot}10^{10}$	$1{\cdot}10^{10}$	$4{\cdot}10^{9}$
12 keV	$2{\cdot}10^{9}$	$7{\cdot}10^{8}$	$2{\cdot}10^{8}$
17 keV	$3{\cdot}10^{8}$	$7{\cdot}10^{7}$	$2{\cdot}10^{7}$

2.4 Future developments: Bragg-Fresnel lenses

The effect of X-ray ($\lambda \sim 1$ Å) focusing by a perfect single crystal with a Fresnel zone structure artificially designed on its surface (a Bragg-Fresnel lens) has recently been studied and experimentally realized by Aristov *et al.*[11]. This class of devices promises to obtain spatial resolutions of the order of .1 μm and, moreover, has already shown good thermal stability under a wiggler beam.

3. SRIXE

A schematic of the SRIXE microprobe is shown in Figure 2. Samples to be analysed (both in air and under vacuum) are mounted on an X–Y–Z translation stage with 1 μm reproducibility. A rotation stage will also be possible. Visualisation of the sample is performed with a zoom microscope and a high resolution camera. The energy dispersive detector (Si(Li)) is positioned in the plane of the storage ring at an angle of 90° to the incident X-ray beam in order to suppress the background due to Compton and Rayleigh scattering. In some cases, this system is limited by the low resolution of solid state detectors (100–200 eV). Use of crystal wavelength-dispersive analysis will be considered for particular applications.

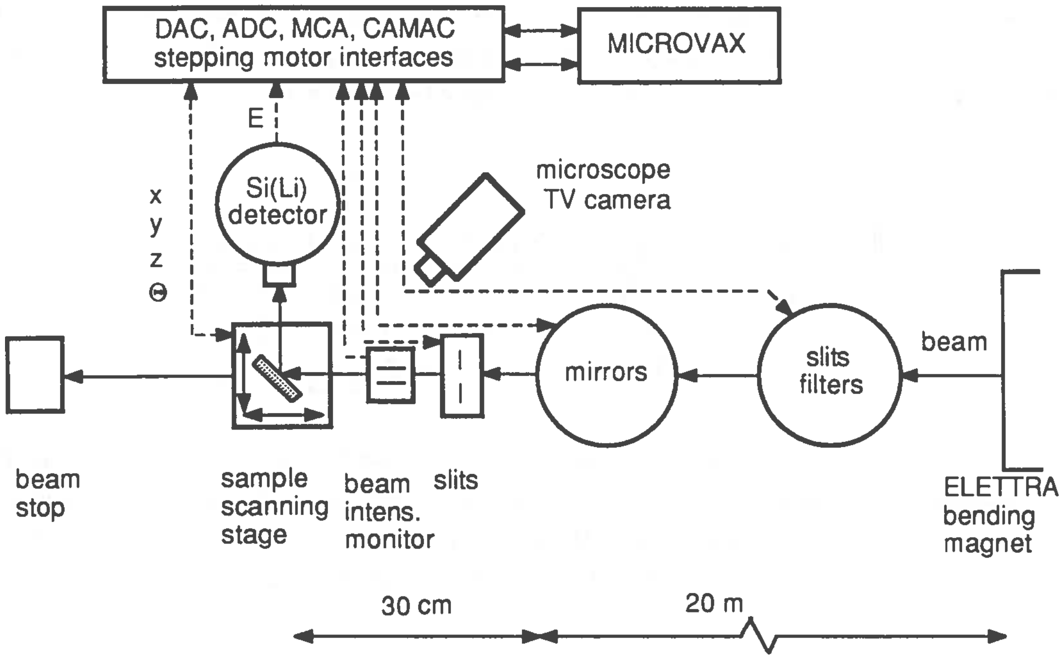

Figure 2. Scheme of the SRIXE and microtomography beamline.

A MicroVAX computer will be used to acquire data in various modes of microprobe operation: single spot analysis, one- or two-dimensional scanning, microtomography (see Section 4). Control of stepping motors for sample translation and rotation stages, and for mirror and slit adjustment will be performed via commercial electronic interfaces.

Finally, the risk of sample contamination from preparation and manipulation (especially at lower levels of analysis) of small and thin biological specimens suggests the use of a clean room environment even during the data acquisition.

A wide band pass system focusing a 10 keV beam of $3 \cdot 10^9$ photons per second on a 100 μm^2 spot has been tested at NSLS by a Berkeley-BNL collaboration[12]. Minimum detectable limits of 3–70 fg were achieved for elements with Z = 19 (K) to 30 (Zn). They inferred minimum detection limits of 1–40 ppm for the same elements present in biological tissue thin sections of mass thickness 1 mg/cm^2 (*e.g.* individual cells). Spatial distribution of trace elements was determined using count intervals of 60 seconds per 10×10 μm pixel.

The performance of the SRIXE system proposed for ELETTRA is given in the following for the detection of Cr, Zn and Sr, elements of interest in biomedical studies.

Using the multilayer coated Kirkpatrick-Baez configuration described in Section 2.3 and using an energy dispersive detector with a solid angle efficiency of 10^{-3}, for 1 $fg/\mu m^2$ Cr, Zn and Sr in a biological sample, the proposed microprobe would produce approximately the counting rates reported in Table V.

Table V. SRIXE counting rates.

Element	Energy	100 μm^2	10 μm^2	1 μm^2
Cr	7 keV	100 cps	25 cps	9 cps
Zn	12 keV	18 cps	6 cps	2 cps
Sr	17 keV	1 cps	0.2 cps	0.1 cps

Sensitivity and spatial resolution should be sufficient to map trace and minor elements in biological cells (as an example, a single erythrocyte has a circular structure with a diameter of about 10 μm). Minimum Detection Limits of 1 - 100 ppm are expected for thin sections (1 mg/cm^2) of biological tissues.

4. Computed microtomography

Computed Microtomography (CMT) with micrometric resolution has become possible with the high photon fluxes available at synchrotron radiation X-ray sources. The filtered radiation from the NSLS X-26 Microprobe beamline has been used to obtain images with a spatial resolution of 30 μm. These experiments show that a resolution of 1 μm could be obtained[13]. In the method of the X-26 group, the sample is scanned at different angles through the X-ray microbeam while the transmitted photons are detected. The lateral resolution is determined by the size of the beam, the scanning interval and the angular increment. The experimental apparatus described in Section 3 can be used with minor modifications as a microtomographic system.

An alternative method was developed at NSLS by the EXXON group[14], based on multislice imaging using a 2-dimensional CCD detector. In this case the resolution is determined by the detector element pitch.

The microbeam from the bending magnet of ELETTRA will be used for transmission tomography, differential tomography and X-ray fluorescence tomography. Magnification techniques and solid-state detector arrays will be studied to increase spatial resolution and minimize measuring time.

5. Applications in life science

There is an increasing demand for high-sensitivity microanalytical methods to determine the metabolic roles of trace elements in biological systems. An important area of current investigation is the correlation between concentrations and distribution of essential and inessential trace elements and the functioning of living systems. Whole body, organ or blood trace element levels are usually measured, but it is expected that the knowledge of the distribution of chemical elements on a microscopic scale in biological systems may be of help in correlating subcellular events with basic morphological or pathological modifications.

Measurements of trace elements at the cellular level relate metals to initiation and development of cancer, cardiovascular dysfunction and other diseases. For example, cells from lymphoma patients showed an increased concentration of titanium, magnesium and zinc[15,16]; titanium and iron were abnormally high in macrophage tumor cells[17].

More recently, elemental profiles of erythrocytes and neutrophil granulocytes from breast cancer patients showed significant alterations in major and trace elements[18]. These analyses were performed with micro-PIXE (proton microbeam of 10 - 100 μm^2) using freeze-dried cells. The elements of interest had a concentration of 1–100 $\mu g/g$ dry tissue.

The X–26 group at NSLS has suggested that *in vivo* analysis with synchrotron radiation can be performed by using cultured cells in a wet specimen holder. Scanning and microtomographic techniques based on transmission, scattering and fluorescence of an X-ray microbeam would determine elemental and density mapping at the cellular level.

The advantage of using X-rays for elemental analysis is that the energy deposited is reduced 10^4-fold for the same MDL achieved with protons and electrons, and the analysis can be performed in air. Still, the use of the X-ray microprobe to study a living cell remains a problem, even in the analysis of major constituents. For example, our 7 keV beam of 1 μm^2 would produce 100 cps in the detector from a potassium concentration of one part per thousand, with an energy deposition of 10^3–10^4 Gy/s, a lethal dose for cells. Isaacson[19] has summarized the available data on the relation between dosage and damage for biological materials. We know that a dose of 10^4 Gy is sufficient to kill every living cell, and that 10^7 Gy induces severe structural damage in most organic specimens, but the composition and structure of the specimen itself, as well as the spatial distribution of the incoming radiation are important parameters.

Moreover, a major effort is needed to understand the correlation between the irradiation and the production of non permanent changes of a living biological material, such as abnormal behaviour of a cell or its membrane and irregular distribution of trace elements. Usually a population of cells is irradiated to determine statistically the damage produced by ionizing radiation. A synchrotron radiation microbeam impinging on a single cell could be used to observe the evolution of this biological microstructure under controlled conditions.

6. Acknowledgements

The group of the X–26 beamline at NSLS was a major source of inspiration for this work. We would also like to acknowledge G. F. Herzog, M. Lovrecich and R. K. Moniot for critical reading of the manuscript, S. Rizzarelli and A. Sedmach for technical support.

7. References

1. A. C. Thompson, J. H. Underwood, Y. Wu, R. D. Giacque, K. W. Jones and M. L. Rivers, *Nucl. Instr. and Meth.* **A266** (1988) 318.
2. K. W. Jones and B. M. Gordon, *Anal. Chem.* **61** (1989) 5.
3. M. R. Howells and J. B. Hastings, *Nucl. Instr. and Meth.* **208** (1983) 379.
4. J. V. Gilfrich, E. F. Skelton, S. B. Odari, J. P. Kirkland and D. J. Nagel, *Anal. Chem.* **55** (1983) 187.
5. A. Iida, K. Sakurai, T. Matsushita and Y. Goshi, *Nucl. Instr. and Meth.* **228** (1985) 659.
6. J. H. Underwood, A. C. Thompson, Y. Wu and R. D. Giauque, *Nucl. Instr. and Meth.* **A266** (1988) 296.
7. J. A. Howells and P. Horowitz, *Nucl. Instr. and Meth.* **125** (1975) 225.
8. P. Kirkpatrick and A. V. Baez, *J. Opt. Soc. Am.* **38** (1948) 766.
9. A. G. Michette, "Optical Systems for Soft X-Rays", Plenum Press, New York (1986) chapt. 4.
10. B. Lai and F. Cerrina, *Nucl. Instr. and Meth.* **A246** (1986) 337; B. Lai, K. Chapman and F. Cerrina, *Nucl. Instr. and Meth.* **A266** (1988) 544.
11. V. V. Aristov, Y. A. Basov, G. N. Kulipanov, V. F. Pindyurin, A. A. Snigirev and A. S. Solokov, *Nucl. Instr. and Meth.* **A274** (1989) 390.
12. R. D. Giacque, A. C. Thompson, J. U. Underwood, Y. Wu, K. W. Jones, M. L. Rivers, *Anal. Chem.* **60** (1988) 855.
13. P. Spanne and M. L. Rivers, *Nucl. Instr. and Meth.* **B24/25** (1987) 1063.
14. B. P. Flannery, H. W. Deckman, W. G. Roberge, K. L. D'Amico, *Science* **237** (1987) 1439.
15. H. Koyama–Ito, A. Jahnke, E. Wada, T. Tsumita and T. Yamazaki *Nucl. Instr. and Meth.* **166** (1979) 595.
16. A. Jahnke, T. Shinmmen, H. Koyama–Ito and T. Yamazaki, *Chemosphere* **10** (1981) 303.
17. H. Koyama–Ito, E. Wada, T. Tsumita, M. Horiuchi and S. Iwata, *Nucl. Instr. and Meth.* **B3** (1984) 625.
18. E. Johansson, U. Lindh, H. Johansson and C. Sundström, *Nucl. Instr. and Meth.* **B22** (1987) 179.
19. R. Isaacson, in "Principles and Techinques of Electron Microscopy", M. A. Hayat (ed.), Van Nostrand Reinhold, New York (1976) vol. 7, 1-78.